Ground Deformation and Damage Assessment using SAR Observations: A Case Study of Hinatuan, Philippines in the 2023 Surigao Del Sur Earthquake

Riva Karyl P. Varela [1, 2]

[1] Caraga State University, Ampayon, 8600 Butuan City, Philippines – rkpvarela@carsu.edu.ph
[2] Université Côte d'Azur, 06200 Nice, France

Keywords: earthquake, InSAR, Sentinel 1, damage assessment, ground deformation

Abstract

Earthquakes are among the major hazards that lead to economic loss every year. Rapid damage assessment is essential for a more efficient disaster response. The 2023 Surigao del Sur earthquake in the Philippines with moment magnitude (Mw) 7.4 occurred on December 2, 2023, with Hinatuan as the nearest municipality located 12 km south of the epicenter. Thus, this study examined the co-seismic impacts in Hinatuan using Synthetic Aperture Radar (SAR) observations. Using phase interferometry and displacement maps to estimate the ground surface deformation, results show that the phase interferograms, Line-of-sight (LOS) displacements, and vertical displacements were consistent, with most of Hinatuan experiencing an uplift of up to 7.2 cm. In contrast, subsidence as low as –9.0 cm was observed in some isolated areas. The damage assessment conducted through change detection analysis revealed 6.15 ha (6.4%) of built area out of the total 84 ha was significantly damaged. The damage mainly occurred in the uplifted regions between 0 to 5 cm. Building codes, land-use planning, and risk management and assessment can be improved and strengthened with these findings for a more earthquake-resilient community. The findings will be a basis for disaster risk reduction and management actions. These may, furthermore, serve as a reference for the development planning of local government units, especially for urban and built-up areas. These can also be used in developing Information, Education, and Communication (IEC) materials and advisory for residents in Hinatuan and the vulnerable adjacent regions.

1. Introduction

Rapid damage assessment is crucial in identifying the possible extent and effects caused by earthquakes. This hazard often results in the loss of lives and infrastructure damage every year. Fast and accurate evaluation of these damages is thus needed as it can aid in prioritizing areas for more efficient performance on disaster response.

The Philippines is a tectonically active area along the Pacific Ring of Fire. With its location, numerous volcanos, faults, and subduction zones have formed throughout the archipelago, resulting in an average of 100 to 150 earthquakes annually, with Mw 4.0 and above (UNOCHA, 2017). One of the major tectonic features is the Philippine Trench, a subduction zone extending to about 1320 km long east of the Philippines and has been tectonically active with a generally reverse faulting motion (Chen et al., 2020). Furthermore, Ramos et al. (2012) determined that at least four large earthquakes greater than Mw 7.5 caused by the Philippine Trench occurred during the last 8000 years. The recent movement along the Philippine Trench was associated with the Mw 7.4 offshore earthquake in Surigao del Sur on December 2, 2023. Over 3000 aftershocks ranging from Mw 1.4 to 6.6 followed the main rupture, with about 528000 people affected (Llamas et al., 2024).

Based on the PHIVOLCS Earthquake Intensity Scale (PEIS), Hinatuan, located 12 km south of the epicenter, has a reported intensity of PEIS VI. This is classified as “Very Destructive,” wherein infrastructures are slightly damaged with limited rockfalls in mountainous areas (PHIVOLCS, 2023). However, 268 houses were reported to be partially damaged, while 90 houses were destroyed in the whole municipality of Hinatuan, along with several government and public buildings (UN OCHA, 2023). The damaged and collapsed infrastructure resulted in an estimated 98.4 million PHP (1.75 million USD) worth of damage (Patumbon, 2023).

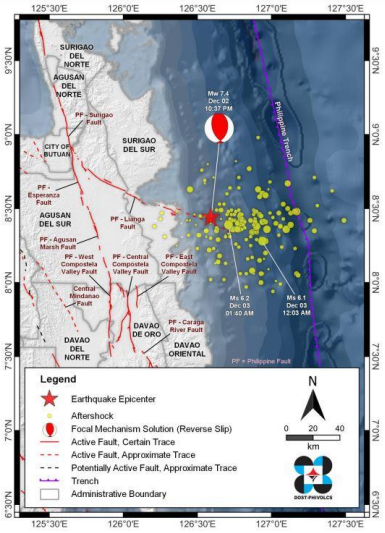

Figure 1. 2023 Surigao del Sur earthquake with main shock epicenter at 08.44°N, 126.59°E and its aftershocks (Source: PHIVOLCS, 2023)

Sentinel- 1 uses active remote sensing that transmits microwave signals and receives these backscattered signals to map the Earth's surface regardless of weather and time conditions. Synthetic Aperture Radar (SAR) uses this imaging system by using short physical antennas to synthesize the effect of a long antenna or short operating wavelength to generate higher-

This contribution has been peer-reviewed. The double-blind peer-review was conducted on the basis of the full paper.
https://doi.org/10.5194/isprs-annals-X-5-2024-213-2024 | © Author(s) 2024. CC BY 4.0 License.

resolution data. Sentinel-1 has been proven helpful in rapidly and accurately detecting and monitoring changes before and after an event. This includes ground deformation caused by earthquakes and other ground movements using the Interferometric Synthetic Aperture Radar (InSAR), which produces a ground deformation map with centimeter-scale accuracy covering a large spatial area (Lillesand et al., 2015).

Studies on surface deformation and post-earthquake damage assessments using SAR data have been widely conducted due to their efficiency and cost-effectiveness in evaluating post-earthquake damage. Du et al. (2024) acquired and evaluated ground deformation during the 2023 Turkey earthquake within only two days, thus providing information for rapid post-earthquake rescue operations. In Nepal, Kumar et al. (2022) utilized C-band SAR data for hazard-risk analysis by combining structural and building damages with built-up land and population to assess the area’s vulnerability. Moreover, SAR observations were used by Zhu et al. (2023) in China to help preserve and protect heritage buildings in earthquake-prone regions by detecting surface fractures in these types of buildings. Recently, Light Detection and Ranging (LiDAR) data were utilized to identify damaged buildings as it provides more detailed information, such as the post-earthquake damage assessments at a building scale as conducted by Saganeiti et al. (2020) in central Italy. However, LiDAR data are scarce, usually collected only during specific circumstances, resulting in limited LiDAR analyses and studies. Despite its long history and applicability, InSAR has only recently been utilized in earthquake deformation assessment studies in the Philippines, such as the vertical displacement assessment during the 2017 Surigao earthquake (Gagula et al., 2022), ground surface deformation mapping of the 2020 Masbate earthquake (Tiongson and Ramirez, 2022; Sta. Rita et al., 2023), and co-seismic deformation delineation during the 2022 Northwestern Luzon earthquake (Perez et al., 2023).

Evaluating the movements of an earthquake and its mechanism is essential in determining and assessing the possible damage of the associated hazards and risks. The results are crucial to land-use planning, policy recommendation, emergency response, and risk management and assessment. These results can also serve as a basis for the development planning by the local government and educational materials among residents in the area.

Thus, using SAR observations, this study examined the co-seismic impacts in Hinatuan during the 2023 Surigao del Sur earthquake. Specifically, it aimed to:

1. Estimate co-seismic vertical ground displacement;
2. Assess the extent of urban damage; and
3. Relate ground deformation and urban damage.

2. Data and Methods

The study utilized Sentinel-1 imageries of Hinatuan acquired during the 2023 Surigao del Sur earthquake. The data was processed using SNAP 9.0, and map layouts were created using ArcGIS Pro 3.2. The generated maps assessed and evaluated the area's ground surface deformation and detected changes during the event. Section 2 describes the study area and how ground deformation and building damage were assessed in this study.

2.1. Study area

Hinatuan is one of the municipalities of Surigao del Sur province in the Philippines, covering an area of 431 km^2 with a population of over 40000 people. The Pacific Ocean bounds it on the east and gentle to moderate elevation mountains on the west. Due to its vast, relatively flat terrains, agricultural activities have contributed significantly to the socio-economic life of the people (Local Government Unit of Hinatuan, 2023). The study area is generally classified into six classes, with trees/forest comprising the largest area with scattered patches of agricultural and built areas throughout, as seen in Figure 2. Due to this, the study focused on Poblacion, which has relatively low vegetation, to reduce errors caused by surface scattering, as well as high built areas and population density in the municipality.

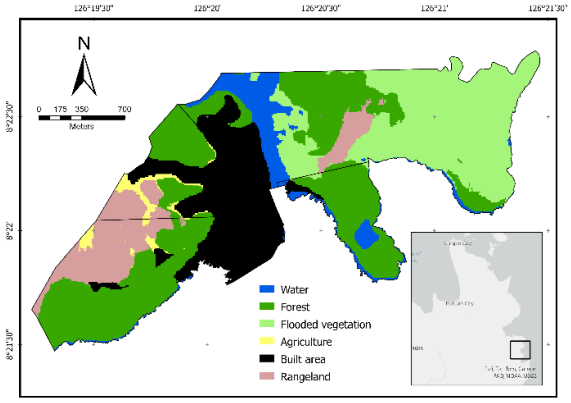

Figure 2. Classified land cover adapted from the 10-m Sentinel-2 L2A 2022 land cover map derived from ESRI (Karra, et al., 2021)

2.2. Surface ground deformation

Co-seismic interferometric pairs were used to denote the slight changes in the relative position of the different points due to the phase difference. These changes were quantified based on the distance relative to the satellite.

2.2.1. Phase interferogram. The study utilized two co-seismic Sentinel-1A Single Look Complex (SLC) C-band imageries acquired from the Alaska Satellite Facility (ASF), capturing data from November 22, 2023, and December 4, 2023, as seen in Table 1. To co-register both images, orbit files and sub-swaths were collected. The study area was limited to bursts 2 and 3 for the vertical polarization of Interferometric Wide (IW) swath 1.

Master image date	22 November 2023
Slave image date	4 December 2023
Path	163
Frame	565
Orbit	Descending
Temporal baseline (days)	12
Spatial baseline (m)	87

Table 1. Co-seismic interferometric pair specification.

The co-registered images were back geocoded using an SRTM 3Sec digital elevation model, producing an interferometric pair. Since multiple bursts were used, Enhanced Spectral Diversity (ESD) and debursting were done to minimize the phase discontinuities, estimate a constant azimuth offset, and remove

the gap between the bursts (Serco Italia SPA, 2019). An interferogram map was produced, displaying fringes with a complete 2π cycle. Phase signatures were emphasized in the interferogram map by removing topography and noise and filtering to enhance the phase unwrapping accuracy while reducing both resolution and size using the multilooking function. However, using SNAPHU to reconstruct the original phase signatures and values and recover definite phase data, phase unwrapping was done. This process allowed a smoother phase field by considering and correcting the phase difference among neighboring pixels (Werner et al, 2002). The Range-Doppler Terrain Correction function shifted proper pixel locations of the interferograms generated to the WGS84/ UTM Zone 51N projection.

2.2.2. Vertical displacement. Displacements relative to the satellite were obtained using the Phase to Displacement tool onto the unwrapped interferogram. A more positive value indicates the ground moving towards the satellite, while a negative value signifies moving away. However, to calculate the ground vertical displacement, Equation 1, derived from Ferretti et al. (2007), was used with the assumption that the motion was purely vertical.

$$Vertical\ displacement = \frac{(unwrapped\ phase\ \times \lambda)}{(-4\pi\ \times \cos\ \theta)} \quad (1)$$

where λ = wavelength
θ = incidence angle

The wavelength for a Sentinel-1 C-band with 5.404 GHz central frequency is 0.0555 m (ESA, 2023). Meanwhile, the incidence angle from the metadata of the Sentinel-1 imagery products is 36.8º. Finally, a reference point was used to compute the absolute vertical displacement. This refers to areas wherein no to little change was experienced and were identified using the coherence map to be highly coherent at 0.02635 m (Ferretti et al., 2007). The reference point value was added to the value from Equation 1 to calculate the final absolute vertical displacement of the area. Positive values are uplifted areas, while negative values are areas that experienced subsidence.

2.3. Damage assessment

Similar to generating phase interferograms, damage assessment using SNAP 9.0 utilized two co-seismic imageries acquired from the Alaska Satellite Facility (ASF). However, Sentinel-1A Ground Range Detected (GRD) C-band from November 22, 2023, and December 4, 2023 were used instead of SLC products. Significant changes due to the earthquake can be easily determined unless there is flooding or large amounts of debris (UN-SPIDER, n.d.). Pre-processing was done by applying orbit files, calibration, speckle filter, terrain correction, and linear conversion. These images were co-registered to produce coherence maps for change detection. The changes were based on the difference in dB values between the images with a threshold of 2. Areas with collapsed buildings have values closer to 2, indicating that the images have distinct differences. Meanwhile, areas with values closer to 0 have significantly similar images; thus, no significant damage was detected.

3. Results

The change detection on ground movement and urban damage in Hinatuan during the 2023 Surigao del Sur earthquake was determined using phase interferograms, vertical displacements, and change detection maps. Section 3 presents the results of the ground deformation and building damage generated in this study.

3.1. Surface ground deformation

Phase changes generated fringes that denote the phase difference during the event. These changes were used to estimate the surface displacements and determine the sense of ground movement.

3.1.1. Phase interferogram. Figures 3 and 4 show the co-seismic phase maps of Hinatuan during the earthquake event. The fringes in these interferometric maps indicate the amount of deformation that has occurred in the area. In Figure 3, no distinct fringe patterns were observed in densely vegetated areas, where intense phase noise is primarily present. However, the northern and southern portions of the built area show distinct fringes. The pattern in these areas suggests a movement towards the satellite, indicating ground uplift.

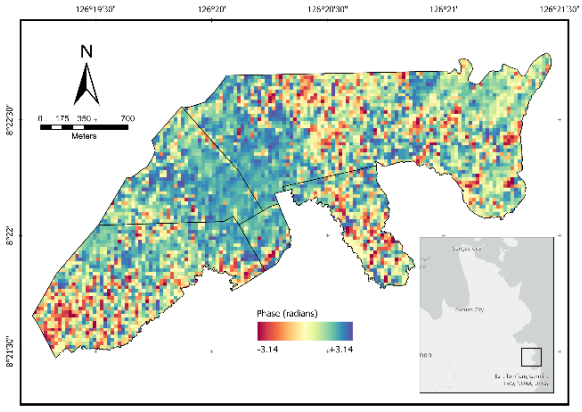

Figure 3. Wrapped interferogram of Hinatuan.

Figure 4 shows areas with distinct phase values, especially within the built areas. Due to the equation used during the data processing done by SNAPHU, positive values in unwrapped interferograms indicate subsidence, while negative values denote uplift. Thus, the northern part of the built areas suggests that the ground experienced an uplift, while the southern part denotes ground subsidence.

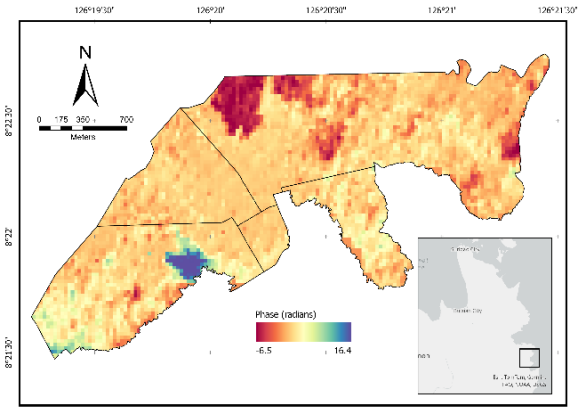

Figure 4. Unwrapped interferogram of Hinatuan.

3.1.2. Vertical displacement. Figures 5 and 6 show the co-seismic displacement maps of Hinatuan during the earthquake. Positive values in red indicate an increase in the ground elevation, while negative values in blue signify a decrease. Figure 5 shows that most of the study area has undergone an increase in elevation with the line-of-sight (LOS) of up to 3.9 cm, with the highest increase being in the northern portion of the built areas. Meanwhile, the greatest subsidence was exhibited along the coast in the southern portion of the built areas, with a decrease of up to -7.2 cm. These observations corresponded with the phase interferograms.

Similarly, Figure 6 shows that the study area experienced an uplift mainly due to an increase in elevation of up to 7.2 cm. Some parts of Hinatuan also underwent subsidence with a ground lowering of up to -9.0 cm in areas along the coast south of the built areas.

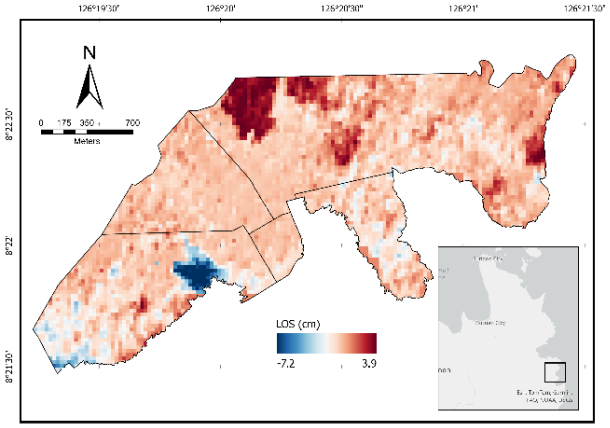

Figure 5. Line-of-sight (LOS) map of Hinatuan.

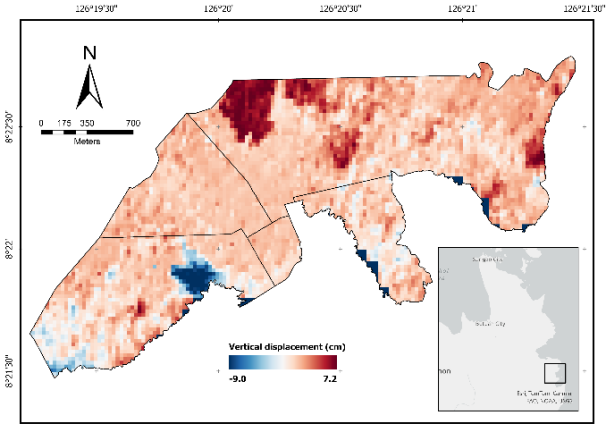

Figure 6. Vertical displacement map of Hinatuan.

3.2. Damage assessment

Figures 7 and 8 show the distribution of the damaged area based on the change detection analysis conducted. The damage is generally scattered throughout the area; however, most of the damage is concentrated along the coast. The built area covers about 84 ha, of which 6.15 ha or 6.4% of the total built area was damaged. The damage mainly occurred in the regions that experienced a vertical displacement of 0 to 5 cm. In comparison, very little damage occurred in either less than -5 cm or more than 5 cm of ground movement, as summarized in Table 2.

Figure 7. Change detection map of damage areas in Hinatuan.

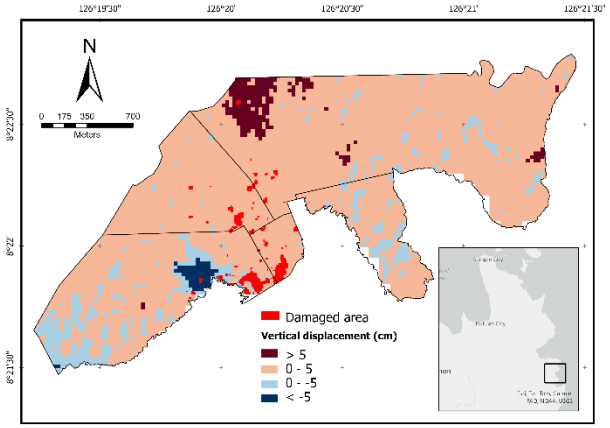

Figure 8. Urban damage distribution along the vertical displacement map of Hinatuan.

Vertical displacement (cm)	Area	
	ha^2	%
< -5	0.08	1.30
-5 to 0	1.52	24.71
0 to 5	4.42	71.87
> 5	0.13	2.11

Table 2. Vertical displacement experienced in the built areas of Hinatuan.

4. Discussion

The ability to assess and estimate the co-seismic displacement and changes during the 2023 Surigao del Sur earthquake using SAR observations was evident when comparing the November 22, 2023 and December 4, 2023 Sentinel-1 imageries. Since the earthquake was offshore, gently sloping ground deformations were expected and observed by the widely spaced interferometric fringes in the generated interferometric maps. However, due to areas with high vegetation canopy in some parts of Hinatuan, decorrelation in the co-seismic pairs, resulting from high phase noise caused by volume scattering, is present. According to Chindo et al. (2022), acquiring InSAR data in humid, tropical environments is challenging due to the heavy vegetation cover. Other factors may also contribute to phase noises, such as temporal change of scatterers, different look angles, and volume scattering. Tiongson and Ramirez (2022) and Sta. Rita et al.

(2023) suggest using multiple pre-seismic and co-seismic event SAR data to minimize the environmental variables present in the area. However, regions that exhibit good coherence can be used for assessment. By examining areas with less noise near the coast, distinct fringes can be observed, indicating areas with good coherency. The behavior of the interferometric fringes and vertical displacement values implies an uplift of up to 7.2 cm was experienced in the area during the event. Meanwhile, areas with vertical displacements of up to -9.0 cm and 7.2 cm, such as those located in the northern and southern parts, respectively, are primarily due to the underlying clastic rocks and limestones present (Aurelio and Peña, 2010). Though the actual fault rupture cannot be observed due to the offshore location of the earthquake, the results obtained in this study coincided with the reverse faulting mechanism of the earthquake.

Rapid assessment of urban damage due to earthquakes based on its relationship to the ground vertical displacement is essential in understanding the structural stability of buildings and other infrastructures in the area. Hinatuan experienced a seemingly small ground displacement; however, SAR observations determined an estimated 6.15 ha of the built area to be significantly damaged. Building damage increases with increasing absolute ground displacement values, resulting in a high intensity of hazard, vulnerability, and risk (Saganeiti et al., 2020; Kumar et al., 2022). Furthermore, a linear and quadratic relationship was identified between co-seismic and building types, wherein reinforced concrete frame structures had the highest seismic capacity compared to other building types (Li et al., 2021).

5. Conclusions

Evaluation of the co-seismic displacement and urban damage during the 2023 Surigao del Sur is essential in detecting, monitoring, and assessing damages due to earthquake ground deformation. The SAR observations indicated the uplifting between 0 to 5 cm in most of the study area, with the highest uplifting at 7.2 cm. However, few places were observed to have subsidence as low as -9.0 cm. These findings coincided with the geodynamics of the area, reverse faulting with Hinatuan lying along the upthrown block. An estimated 6.15 ha of built area in Poblacion has been significantly damaged, making up 6.4%. The damaged regions mainly occurred in uplifted areas between 0 to 5 cm.

More extensive damage estimation and evaluation can be done by reducing phase noises and decor-related areas using more pre-seismic, co-seismic, and post-seismic data or considering smaller baselines. More powerful penetrating radars, such as L-bands or P-bands, should be utilized to penetrate through the thick forest covers. Lastly, detailed individual building characterization, damage assessment, and validation would be beneficial. The findings will then be an essential basis for development planning, disaster risk reduction management, and emergency response in vulnerable areas such as Hinatuan and the nearby regions. These will also serve as useful inputs in developing Information, Education, and Communication (IEC) materials and advisory for residents in Hinatuan and the adjacent vulnerable areas.

References

Aurelio, M.A. & Peña, R.E. (2010). Geology of the Philippines, 2nd Edition. Quezon City, Philippines: Mines and Geosciences Bureau, Department of Environment and Natural Resources. 532.

Chen, P. F., Chien, M., Bina, C. R., Yen, H. Y., & Olavere, E. A. (2020). Evidence of an east-dipping slab beneath the southern end of the Philippine Trench (1 N–6 N) as revealed by ISC-EHB. Journal of Asian Earth Sciences: X, 4, 100034.

Chindo, M., Hashim, M., & Rasib, A. (2022). Interferometric synthetic aperture radar coherence constraints in heavily vegetated tropics. IOP Conference Series: Earth and Environmental Science. 1064, p. 12027. IOP Publishing.

Du, Y. N., Feng, D. C., & Wu, G. (2024). InSAR-based rapid damage assessment of urban building portfolios following the 2023 Turkey earthquake. International Journal of Disaster Risk Reduction, 104317.

ESA. (2023). Copernicus: Sentinel-1. Retrieved December 18, 2023, from eoPortal: https://www. eoportal.org/satellite-missions/copernicus-sentinel-1

Ferretti, A., Monti-Guarnieri, A., Prati, C., & Rocca, F. (2007). InSAR Principles: Guidelines for SAR. The Netherlands: European Space Agency Publications.

Gagula, A., Bolanio, B. P., Bermoy, M. M., Bisnar, T. M., & Bolatete, M. A. (2022). Integrating GIS and Earth Observation Data in Assessing Land Subsidence Caused by Large Seismic Movements: A Case Study in Surigao City, Mindanao, Philippines. 43rd Asian Conference on Remote Sensing (ACRS2022). 2, p. 1062. Ulaanbaatar, Mongolia: Asian Association on Remote Sensing (AARS).

Karra, K., Kontgis, C., Statman-Weil, Z., Joseph, C., Mathis, M., & S.P., B. (2021). Global land use/land cover with Sentinel-2 and deep learning. IEEE IGARSS 2021. Brussels, Belgium: IEEE International Geoscience and Remote Sensing Symposium.

Kumar, A., Lal, P., Prasad, A., Tripathy, P., & Saikia, P. (2022). Analyzing urban damage and surface deformation based hazard-risk in Kathmandu city occurred during Nepal earthquake (2015) using SAR interferometry. Advances in Space Research, 70(12), 3892-3904.

Li, Q., Wang, W., Wang, J., Zhang, J., & Geng, D. (2021). Exploring the relationship between InSAR coseismic deformation and earthquake-damaged buildings. Remote Sensing of Environment, 262, 112508.

Lillesand, T., Kiefer, R. W., & Chipman, J. (2015). Remote sensing and image interpretation (7th ed.). Hoboken, New Jersey, USA: John Wiley & Sons.

Llamas, D., Perez, J., Legaspi, C., Acid, J., & Naing, J. (2024). Understanding the December 2023 Earthquakes in Eastern Mindanao, Philippines: What Happened and Why It Matters. Quezon City: PHIVOLCS Open-File Report No. 24-01.

Local Government Unit of Hinatuan. (2023). About the Municipality of Hinatuan. Retrieved March 29, 2024, from Local Government Unit of Hinatuan: https://visithinatuan. com/about-hinatuan/

Patumbon, R. G. G. (2023). P98.4-M quake damage in Hinatuan, Surigao Sur. SunStar Publishing Inc. Retrieved on March 29, 2023 from: https://www.sunstar.com.ph/davao/ p984-m-quake-damage-in-hinatuan-surigao-sur

Perez, J.S., Llamas, D.C.E., Dizon, M.P., Buhay, D.J.L., Legaspi, C.J.M., Lagunsad, K.D.B., Constantino, R.C.C., De Leon, R.J.B., Quimson, M.M.Y., Grutas, R.N., & Pitapit, R.S.D. (2023). Impacts and causative fault of the 2022 magnitude (Mw) 7.0 Northwestern Luzon earthquake, Philippines. Frontiers in Earth Science, 11, 132.

PHIVOLCS. (2023, December 3). Primer on the 02 December 2023 Magnitude (Mw) 7.4 Offshore Surigao Del Sur Earthquake. Retrieved December 18, 2023, from Philippine Institute of Volcanology and Seismology: https://www. phivolcs.dost.gov.ph/index.php/news/21463-primer-on-the-02-december-2023-magnitude-mw-7-4-offshore-surigao-del-sur-earthquake

Ramos, N., Tsutsumi, H., Perez, J., & Bermas Jr, P. (2012). Uplifted marine terraces in Davao Oriental Province, Mindanao Island, Philippines and their implications for large prehistoric offshore earthquakes along the Philippine trench. Journal of Asian Earth Sciences, 45, 114-125.

Saganeiti, L., Amato, F., Nolè, G., Vona, M., & Murgante, B. (2020). Early estimation of ground displacements and building damage after seismic events using SAR and LiDAR data: The case of the Amatrice earthquake in central Italy, on 24th August 2016. International Journal of Disaster Risk Reduction, 51, 101924.

Serco Italia SPA. (2019). Earthquake Deformation Using InSAR, with Sentinel-1. Retrieved December 10, 2023, from RUS Lectures: https://eo4society.esa.int/wp-content/uploads/ 2022/01/HAZA05_EarthquakeDeformation_Hawaii.pdf

Sta. Rita, K., Valkaniotis, S., & Lagmay, A. (2023). Surface Rupture Kinematics of the 2020 Mw6. 6 Masbate (Philippines) Earthquake determined from Optical and Radar Data. EGUsphere, 1-37.

Tiongson, S. F., & Ramirez, R. (2022). Mapping of ground surface deformations and its associated damage using SAR interferometry: a case study of the 2020 Masbate earthquake. E3S Web of Conferences, 347, 3014.

UN Office for the Coordination of Humanitarian Affairs. (2017, May 4). Philippines: Seismic Events in April 2017. Retrieved December 14, 2023, from ReliefWeb: https://reliefweb.int/map/philippines/philippines-seismic-events-april-2017

UN Office for the Coordination of Humanitarian Affairs. (2023). Philippines: 7.4 Earthquake Hinatuan, Surigao Del Sur - Flash Update No.1, As of 03 December 2023, 7 p.m. local time - Philippines. Retrieved March 30, 2024, from ReliefWeb: https://reliefweb.int/report/philippines/philippines -74-earthquake-hinatuan-surigao-del-sur-flash-update-no1-03-december-2023-7-pm-local-time

UN-SPIDER (n.d.) In detail: Earthquake urban damage detection using Sentinel-1 data, UN-SPIDER Knowledge Portal. Retrieved March 25, 2024 from https://www.un-spider.org/advisory-support/recommended-practices/ earthquake-damage-detection-sentinel-1/in-detail

Werner, C., Wegmüller, U., Strozzi, T., & Wiesmann, A. (2002, June). Processing strategies for phase unwrapping for INSAR applications. In proceedings of the European conference on synthetic aperture radar (EUSAR 2002) (Vol. 1, pp. 353-356).

Zhu, M., Chen, F., Fu, B., Chen, W., Qiao, Y., Shi, P., Zhou, W., Lin, H., Liao, Y., & Gao, S. (2023). Earthquake-induced risk assessment of cultural heritage based on InSAR and seismic intensity: A case study of Zhalang temple affected by the 2021 Mw 7.4 Maduo (China) earthquake. International Journal of Disaster Risk Reduction, 84, 103482.